Degeneracies of particle and nuclear physics uncertainties in neutrinoless $\beta\beta$ decay

E. Lisi,[1] A. M. Rotunno,[2] and F. Šimkovic[3,4,5]

[1]*Istituto Nazionale di Fisica Nucleare, Sezione di Bari, Via Orabona 4, 70126 Bari, Italy*
[2]*Dipartimento Interateneo di Fisica "Michelangelo Merlin," Via Amendola 173, 70126 Bari, Italy*
[3]*Department of Nuclear Physics and Biophysics, Comenius University, Mlynská dolina F1, SK–842 15 Bratislava, Slovakia*
[4]*Bogoliubov Laboratory of Theoretical Physics, JINR, 141980 Dubna, Moscow Region, Russia*
[5]*Czech Technical University in Prague, CZ-12800 Prague, Czech Republic*

(Received 19 June 2015; published 5 November 2015)

Theoretical estimates for the half-life of neutrinoless double beta decay ($0\nu\beta\beta$) in candidate nuclei are affected by both particle and nuclear physics uncertainties, which may complicate the interpretation of decay signals or limits. We study such uncertainties and their degeneracies in the following context: three $0\nu\beta\beta$ nuclei of great interest for large-scale experiments (^{76}Ge, ^{130}Te, ^{136}Xe), two representative particle physics mechanisms (light and heavy Majorana neutrino exchange), and a large set of nuclear matrix elements (NME), computed within the quasiparticle random phase approximation (QRPA). It turns out that the main theoretical uncertainties, associated with the effective axial coupling g_A and with the nucleon-nucleon potential, can be parametrized in terms of NME rescaling factors, up to small residuals. From this parametrization, the following QRPA features emerge: (1) the NME dependence on g_A is milder than quadratic, (2) in each of the two mechanisms, the relevant lepton number violating parameter is largely degenerate with the NME rescaling factors, and (3) the light and heavy neutrino exchange mechanisms are basically degenerate in the above three nuclei. We comment on the challenging theoretical and experimental improvements required to reduce such particle and nuclear physics uncertainties and their degeneracies.

DOI: 10.1103/PhysRevD.92.093004 PACS numbers: 21.60.Jz, 14.60.Pq, 14.60.St

I. INTRODUCTION

The search for the neutrinoless mode of double beta decay ($0\nu\beta\beta$) in different (Z, A) candidate nuclei,

$$(Z, A) \to (Z + 2, A) + 2e^-, \tag{1}$$

represents a major research program in experimental neutrino physics [1–5]. From the theoretical viewpoint, this decay mode provides a unique probe of the Dirac or Majorana nature of neutrinos [6] and, in general, of lepton number violation (LNV) processes [7–10]. Indeed, the decay may be mediated not only by Majorana neutrinos with light (sub-eV) masses, but also by other LNV mechanisms involving new particle physics at higher mass or energy scales [6–10].

For a single LNV mechanism (labeled by the index j) occurring in a candidate nucleus (labeled by the index i), the $0\nu\beta\beta$ decay half-life T_i can be expressed as

$$T_i^{-1} = G_i^j |M_i^j|^2 (\lambda^j)^2, \tag{2}$$

where G_i^j is a kinematical phase-space factor, M_i^j is the nuclear matrix element (NME) encoding the nuclear dynamics of the process, and λ^j is a LNV parameter encoding the particle physics aspects of decay. In principle, by means of independent $0\nu\beta\beta$ decay observations in different nuclei, one may hope to disentangle the underlying particle physics mechanism and the associated λ^j value [11–16]. Unfortunately, the relatively large nuclear model uncertainties affecting M_i^j [17–19] make this program quite difficult in practice.

Several studies have investigated the stringent conditions on the M_i^j uncertainties, under which various particle physics mechanisms may—or may not—be disentangled with future, multi-isotope $0\nu\beta\beta$ decay data (see [7,11–16,20–25] for an incomplete bibliography). A new twist in this field has been provided by recent discussions on the axial coupling g_A, which could be significantly suppressed with respect to the vacuum value $g_A^{\rm vac} \simeq 1.27$, due to nuclear medium and other "quenching" effects. In particular, g_A values in the reference range often used in the past literature (see, e.g., [26,27]),

$$1 \lesssim g_A \lesssim 1.27, \tag{3}$$

are being increasingly questioned by phenomenological studies. In fact, in the framework of the quasiparticle random phase approximation (QRPA), best-fit values $g_A < 1$ were obtained in [28] by a joint analysis of the experimental data available for the electron capture (EC),

single beta (β) and two-neutrino double beta ($2\nu2\beta$) processes in the ^{100}Mo and ^{116}Cd nuclei.

For the same weak processes and nuclei, such early indications for $g_A < 1$ [28] were later confirmed in another QRPA approach [29]. Recently, a marked preference for values of g_A below unity has also been found in a different approach based on the interacting boson model (IBM) [30–32], where a possible dependence of g_A on the atomic number has been noted [30]. See also [33] for a recent discussion of quenching variations in the chiral effective field theory approach. In the absence of a deep theoretical understanding of quenching effects [2,27], these findings suggest that the usual reference range in Eq. (3) should be conservatively extended somewhat below unity, e.g., in the range $0.8 \lesssim g_A \lesssim 1.27$ [34].

In general, small (or uncertain) values of g_A may strongly affect the half-life estimates via $T_i^{-1} \propto |M_i^j|^2 \propto g_A^4$, thus making even more difficult to constrain the particle physics mechanism and its LNV parameter [35,36]. However, in the adopted QRPA framework [37], the g_A-dependence of $|M_i^j|$ is known to be *milder* than quadratic, since g_A variations may be partly traded by shifts of another free parameter—the particle-particle strength g_{pp} [38]—via a joint fit to reference $2\nu\beta\beta$ data; see, e.g., [27,28,34,38,39]. Therefore, it makes sense to revisit the problem of determining the particle physics mechanism and its LNV parameter, by allowing $g_A < 1$ within the QRPA.

To this purpose, we consider in the following three nuclei (^{76}Ge, ^{130}Te, ^{136}Xe) and two $0\nu\beta\beta$ mechanisms mediated by light (L) and heavy (H) Majorana neutrino exchange, within an updated QRPA approach. We show that, even if the decay half-lives were accurately measured, the current nuclear model uncertainties (mainly related to g_A and to the nucleon-nucleon potential) would lead to a degeneracy between the LNV parameter and the NME errors in each mechanism, as well as between the mechanisms themselves. Although limited to a few representative nuclei and $0\nu\beta\beta$ decay processes, these results highlight the severe conditions and the challenging improvements needed to (partially) lift such degeneracies in the future.

Our work is structured as follows. In Sec. II we introduce the notation and conventions for the two (L and H) decay mechanisms. In Sec. III we discuss the QRPA calculation of the nuclear matrix elements and the parametrization of the associated uncertainties. In Sec. IV we perform a statistical analysis of prospective data, showing the degeneracy of particle and nuclear physics uncertainties, both within each mechanism and between the two mechanisms. We briefly summarize our results in Sec. V.

II. LIGHT AND HEAVY NEUTRINO EXCHANGE: NOTATION AND CONVENTIONS

In the following, we shall study $0\nu\beta\beta$ decay in three representative nuclei of great interest for large-mass projects,

$$i = 1, 2, 3 = {}^{76}\mathrm{Ge}, {}^{130}\mathrm{Te}, {}^{136}\mathrm{Xe}, \tag{4}$$

and two reference LNV mechanisms, mediated by either light (L) or heavy (H) Majorana neutrino exchange [40,41],

$$j = 1, 2 = L, H. \tag{5}$$

We refer the reader to [7–10] for recent discussions of the particle physics dynamics of the L and H mechanisms, and to [42] for an approach interpolating between these two cases.

Here we just remind that, for the L mechanism, the LNV parameter can be expressed as [1]

$$\lambda^L = m_{\beta\beta} = \left| \sum_{h=1}^{3} |U_{eh}|^2 e^{i\phi_h} m_h \right|, \tag{6}$$

where m_h are the masses of the three known light neutrinos ν_i, U_{eh} are their mixing matrix elements with ν_e, and ϕ_h are unconstrained Majorana phases (one of which can be rotated away). For the H mechanism, the LNV parameter can be expressed as (see, e.g., [41])

$$\lambda^H = M_{\beta\beta} = m_e \left| \sum_{k\geq 4} |U_{ek}|^2 e^{i\Phi_k} \frac{m_p}{M_k} \right|, \tag{7}$$

where M_k are the masses of possible heavy neutrinos beyond the known ones (assuming $M_k \gg m_p$), U_{ek} are their mixing matrix elements with ν_e, and Φ_k are further Majorana phases.

The L and H mechanisms are characterized by the same phase space [41],

$$G_i^L = G_i^H \equiv G_i, \tag{8}$$

which, in the conventions of [37], embeds a factor $1/m_e^2$, so that its units are $[G_i] = y^{-1}\ \mathrm{eV}^{-2}$, while $[\lambda^j] = \mathrm{eV}$.

Finally, we linearize Eq. (2) by taking logarithms as in [13,17,20],

$$\tau_i = \gamma_i - 2\eta_i^j - 2\mu^j, \tag{9}$$

where

$$\tau_i = \log_{10}(T_i/\mathrm{y}), \tag{10}$$

$$-\gamma_i = \log_{10}[G_i/(y^{-1}\ \mathrm{eV}^{-2})], \tag{11}$$

$$\eta_i^j = \log_{10}|M_i^j|, \tag{12}$$

$$\mu^j = \log_{10}(\lambda^j/\mathrm{eV}). \tag{13}$$

Table I reports the numerical values of G_i (and of γ_i) as taken from [43], together with the most stringent

TABLE I. Phase space values [43] and 90% C.L. half-life limits for the three nuclei considered in this work. See the text for details.

i	G_i (y^{-1} eV^{-2})	γ_i	T_i (y)	Experiments
^{76}Ge	2.21×10^{-26}	25.656	$>3.0 \times 10^{25}$	GERDA + IGEX + HdM [44]
^{130}Te	1.33×10^{-25}	24.876	$>4.0 \times 10^{24}$	CUORE-0 + CUORICINO [47]
^{136}Xe	1.36×10^{-25}	24.865	$>3.4 \times 10^{25}$	KamLAND-Zen + EXO-200 [49]

experimental lower limits for the half-lives T_i as quoted by GERDA [44] for ^{76}Ge (in combination with IGEX [45] and HdM [46]), by CUORE [47] for ^{130}Te (in combination with CUORICINO [48]), and by KamLAND-Zen [49] for ^{136}Xe (in combination with EXO-200 [50]). Note that the G_i values of [43] have been rescaled by the fourth power of 1.27, for consistency with our conventions [see Eq. (14) below].

We emphasize that, although the L and H mechanisms share the same phase-space factor G_i, their dynamics is quite different. The exchange potentials behave like $1/r$ and delta functions in the L and H cases, respectively, inducing significant differences in the multipole decomposition of the corresponding matrix elements, as well as in their sensitivity to g_A changes (not shown). Furthermore, the H mechanism is more sensitive than the L one to the choice of the nucleon-nucleon potential (see Sec. III B). Given these intrinsic dynamical differences, one does not expect a priori that the L and H mechanisms are phenomenologically degenerate, as they turn out to be.

III. QRPA NUCLEAR MATRIX ELEMENTS AND UNCERTAINTIES

A. Nuclear matrix elements

The $0\nu\beta\beta$ nuclear matrix element $M = M_i^j$ consists of the Fermi (F), Gamow-Teller (GT) and tensor (T) parts which, in the adopted conventions, read [37,51,52]:

$$M = \left(\frac{g_A}{1.27}\right)^2 \left(-\frac{M_{\rm F}}{(g_A)^2} + M_{\rm GT} - M_{\rm T}^j\right). \qquad (14)$$

Note that the effective axial coupling g_A enters not only in the prefactor and in the Fermi matrix element, but also in the calculation of the GT and tensor constituents, due to a consideration of the nucleon weak-magnetism terms [41].

In this work, six sets of nuclear matrix elements M_i^j have been calculated for each of the three nuclei in Eq. (4) and of the two mechanisms in Eq. (5). In particular, for both light and heavy neutrino mass mechanisms, the calculation is based on the QRPA with partial restoration of isospin symmetry [53]. The nuclear radius $R = r_0 A^{1/3}$ with $r_0 = 1.2$ fm is used. For each pair (i, j), the NME set includes 18 variants, according to three different sizes of the single-particle space (small, intermediate, large), two different types of nucleon-nucleon interaction (charge-dependent (CD) Bonn and Argonne) [52], and three different values of g_A,

$$g_A = 1.27, 1.00, 0.80, \qquad (15)$$

which are representative of unquenched, quenched, and strongly quenched axial couplings. We remind that, for each calculation, the g_{pp} value is fixed by imposing that the corresponding (theoretical) $2\nu\beta\beta$ half-life equals the experimental one in each nucleus [37,51]. Summarizing, the following analysis is based on a total of 108 $0\nu\beta\beta$ matrix elements, calculated within a QRPA framework which reproduces three $2\nu\beta\beta$ half-lives by construction.

Figure 1 shows the scatter plots of these 108 NME values in logarithmic scale, which visualize the correlations between pairs of the η_i^j parameters in Eq. (12). NME variants are distinguished by different marker types: blue and red for L and H mechanisms, full and hollow for Argonne and CD-Bonn potentials, and squares, circles and triangles for $g_A = 0.80$, 1.00 and 1.27, respectively. Single-particle space sizes are not explicitly distinguished (see also below). Note that, for graphical convenience, the M_i^j values for the L mechanism have been multiplied by a factor 100. This figure reveals a very strong correlation of the NME's, which is especially evident in the plane charted by ^{136}Xe and ^{130}Te. In practice, it appears that the theoretical uncertainties associated to NME variants can be largely absorbed by overall scaling factors.

The strong correlations emerging in Fig. 1 imply two different types of degeneracies between nuclear and particle physics aspects of the decay, at least in the (i, j) sets considered herein: (a) for a given decay mechanisms, the nuclear model uncertainties are degenerate with the LNV parameter λ^j [17], and (b) the two different mechanisms (L and H) are largely degenerate with one another [20]. With respect to [17,20], we sharpen these statements by using a convenient parametrization and statistical treatment of the NME uncertainties within the QRPA (including cases with $g_A < 1$), as discussed below.

A final remark is in order. Variations of the single-particle space size (from small to intermediate and large size) produce relatively small NME changes, partly orthogonal to the main degeneracy directions of Fig. 1. These changes do not reveal a specific pattern; e.g., it turns out that, for ^{76}Ge, the NMEs are slightly low for intermediate space size (with respect to small or large sizes), while the opposite happens for ^{130}Te and ^{136}Xe. For the latter two nuclei, the NMEs values for small and large sizes differ somewhat, while they are rather close for ^{76}Ge. In the absence of a compelling pattern emerging from different

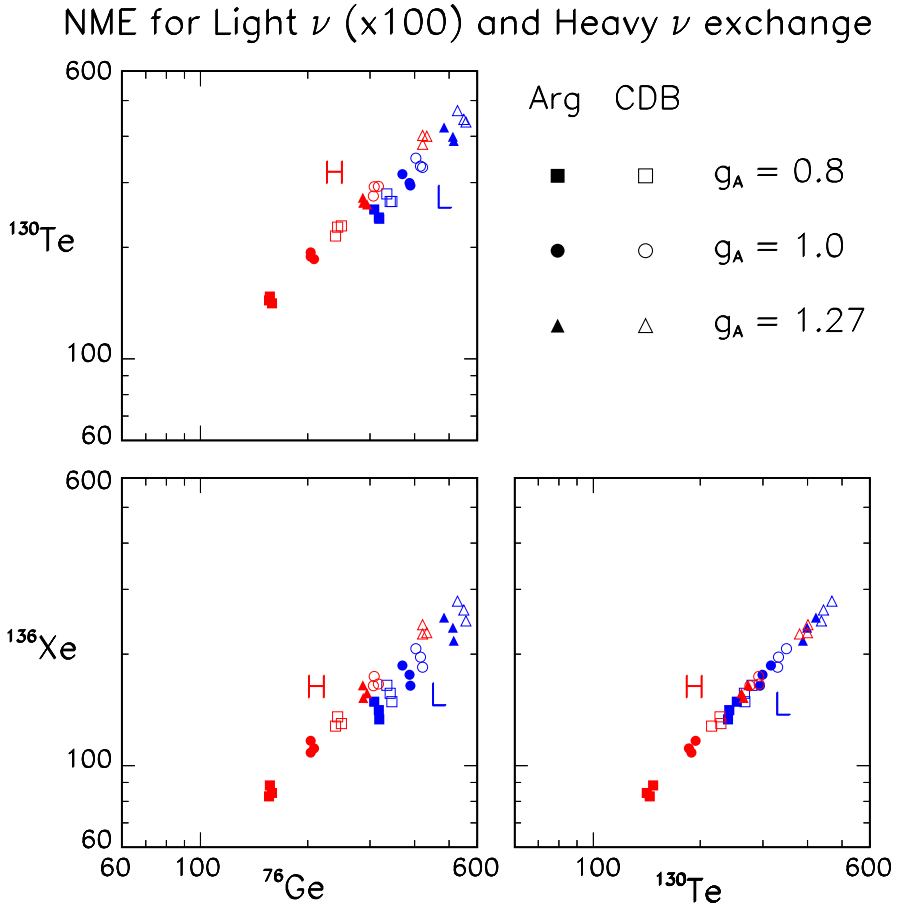

FIG. 1 (color online). Scatter plot (in logarithmic scale) of the nuclear matrix elements $|M_i^j|$, for each pair of the three $0\nu\beta\beta$ candidate nuclei, and for both heavy (H) and light (L) Majorana neutrino exchange. In the latter case, the NME have been multiplied by a factor 100. See the text for details.

single-particle space sizes, we omit their distinction in Fig. 1, and adopt the conservative viewpoint that the associated NME variations are basically uncorrelated among the three nuclei.

B. Parametrization of uncertainties

We find that the spread of the numerical η_i^j values can be fully covered by the following empirical parametrization, which incorporates both the strong linear correlation among the η_i^j and the residual transverse scatter visible in Fig. 1:

$$\eta_i^j = \bar{\eta}_i^j + \alpha^j(g_A - 1) + s\beta^j \pm \sigma^j, \tag{16}$$

where $s = +1$ (-1) for the CD-Bonn (Argonne) potential, and the parameters $\bar{\eta}_i^j$, α^j, β^j and σ^j are given in Table II. In the above equation, $\bar{\eta}_i^j$ represents a sort of "central value" for the set of η_i^j values, while $\alpha^j(g_A - 1) + s\beta^j$ represents the systematic theoretical bias due to admissible variations of g_A with respect to the unit value, and of the nucleon-nucleon potential. In terms of NMEs ($|M| = 10^\eta$), the bias acts as an overall (i-independent) NME rescaling factor for the three nuclei. Finally, $\pm\sigma^j$ represents the residual range which is not covered by the previous bias, including variations due to the basis size (small, intermediate, large). [Actually, the σ^j values covering the η_i^j spread depend slightly on the index i; we neglect these tiny variations, and conservatively take the largest value for σ^j.]

The above parametrization indicates that, within the QRPA, the functional dependence of the $0\nu\beta\beta$ NME on g_A is significantly milder than the naive quadratic expectations ($|M_i^j| \propto g_A^2$), as already noticed in [28,38,39]. We recall that, within the QRPA approach, the g_{pp} parameter is adjusted to fit the $2\nu\beta\beta$ decay rate, and that both the $0\nu\beta\beta$ and $2\nu\beta\beta$ NME ($M^{0\nu}$ and $M^{2\nu}$) decrease with decreasing g_A or with increasing g_{pp}. Then, if g_A decreases, the g_{pp} parameter must decrease as well, in order to keep $M^{2\nu}$ at the value fixed by the $2\nu\beta\beta$ half-life $T^{2\nu}$, as shown in Fig. 2. As a consequence, also the change in the matrix element $M^{0\nu}$ is smaller than one might at first expect (see, e.g., [28]). In particular, Eq. (16) suggests that, for $0\nu\beta\beta$ decay, the effective NME dependence on g_A is close to be linear ($|M_i^j| \propto g_A$) rather than quadratic, at least for relatively small values of the difference $g_A - 1$, and within the rough

TABLE II. Numerical values for the empirical parametrization of nuclear model uncertainties in Eq. (16), for the two L and H mechanisms.

j	$\bar{\eta}_1^j$	$\bar{\eta}_2^j$	$\bar{\eta}_3^j$	α^j	β^j	σ^j
L	0.600	0.504	0.267	0.458	0.021	0.032
H	2.400	2.364	2.135	0.544	0.089	0.025

approximation $\alpha^j \sim 1/2 \sim \ln(10)$. In this sense, the impact of the large g_A uncertainties in the interpretation of $0\nu\beta\beta$ data [30,35,36] may be effectively reduced (although not eliminated) within the QRPA approach [27,28,34].

We remark that, for the sake of simplicity, g_A has been assumed to be the same in the three considered nuclei. This seems to be an acceptable starting point for a phenomenological analysis, since the origin and amount of quenching are not well known. For instance, quenching effects might be assigned to the Δ-isobar admixture in the nuclear wave function, or to the shift of the GT strength to higher excitation energies due to short-range tensor correlations. Model-space truncation can also exclude strength that may be pushed to high energies, and the omission of two-body currents can also leave excitations unaccounted for. Moreover, quenching effects might be different for different multipoles and, if associated with exchange currents, might be smaller for light nuclei. In the absence of a clear picture for these effects, we have assumed that the same value of g_A (either 0.8, 1.0, or 1.27) applies to all multipoles in the three medium-heavy nuclei consider herein. Of course, this simplified assumption may be revisited in future and more refined analyses of the quenching phenomenon within the $0\nu\beta\beta$ decay context. In perspective, one should build a general theory of quenching in the nuclear medium, and constrain systematically the theory with data from different nuclear processes linked to $0\nu\beta\beta$ decay, so as to reduce the effects of the g_A uncertainty (see, e.g., the discussion in [19,54]). At present, however, we must accept theoretical uncertainties (at least) as large as in Eq. (16).

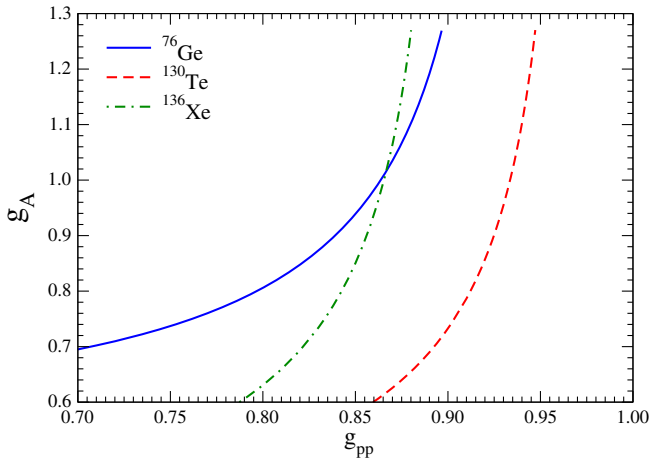

FIG. 2 (color online). The relation between the weak axial-vector coupling parameter g_A and the g_{pp} parameter, determined from the measured $2\nu\beta\beta$ half-life of ^{76}Ge, ^{130}Te and ^{136}Xe. The results refer to the case with Argonne potential and small size for the single-particle model space. Similar results hold for other choices of the potential or model space (not shown).

So far, we have mainly discussed the sensitivity to g_A variations, characterized by the α^j parameters. Let us now comment on the other parameters β^j and σ^j. The value of β^j, which characterizes the NME sensitivity to the choice of the nucleon-nucleon potential, turns out to be much larger in the H mechanism than in the L one (by a factor of about four), as anticipated at the end of Sec. II. Following the remarks at the end of Sec. III A, the theoretical uncertainty $\pm\sigma^j$ is treated as a "one-standard-deviation range," covering those residual uncertainties (including the single-particle space ones) which are not included in the "bias" term $\alpha^j(g_A - 1) + s\beta^j$. This definition is conservative, because it allows us to cover [via Eq. (16)] all the NME in Fig. 1, and not only 68% of them.

C. Degeneracies in terms of observable half-lives

The results of Sec. III B allow us to visualize the degeneracies mentioned at the end of Sec. III A in terms of observable quantities, i.e., the $0\nu\beta\beta$ decay half-lives T_i expected in different nuclei and for different underlying mechanisms. Since the T_i are usually represented in logarithmic scale, we shall base our discussion directly on $\tau_i = \log_{10}(T_i/\mathrm{y})$. From Eqs. (9) and (16), the τ_i can be expressed as

$$\tau_i = \gamma_i - 2\bar{\eta}_i^j - 2\bar{\mu}^j \pm 2\sigma^j, \tag{17}$$

where we have defined a "rescaled" LNV parameter $\bar{\mu}^j$ as

$$\bar{\mu}^j = \mu^j + \alpha^j(g_A - 1) + s\beta^j. \tag{18}$$

The above equations clearly show the degeneracy between the particle physics parameter μ^j and the systematic QRPA uncertainties parametrized by $\alpha^j(g_A - 1) + s\beta^j$: variations of the latter term can be traded for opposite changes in the LNV parameter, without affecting the observable τ_i.

Figure 3 shows the theoretical expectations in the planes charted by pairs of half-lives (τ_k, τ_h) in different nuclei, together with the current experimental lower limits as reported in Table I. The half-lives are correlated via Eq. (17), which implies

$$\tau_k - \tau_h = \gamma_k - \gamma_h - 2(\bar{\eta}_k^j - \bar{\eta}_h^j) \tag{19}$$

for $j = H, L$, up to residual errors ($\pm 2\sigma^j$), shown as crosses in Fig. 1. The position of each cross is irrelevant: the associated errors are the same at any point on the slanted lines—which should thus be thought of as "error bands." This figure illustrates the second kind of degeneracy mentioned at the end of Sec. III B, namely, the near

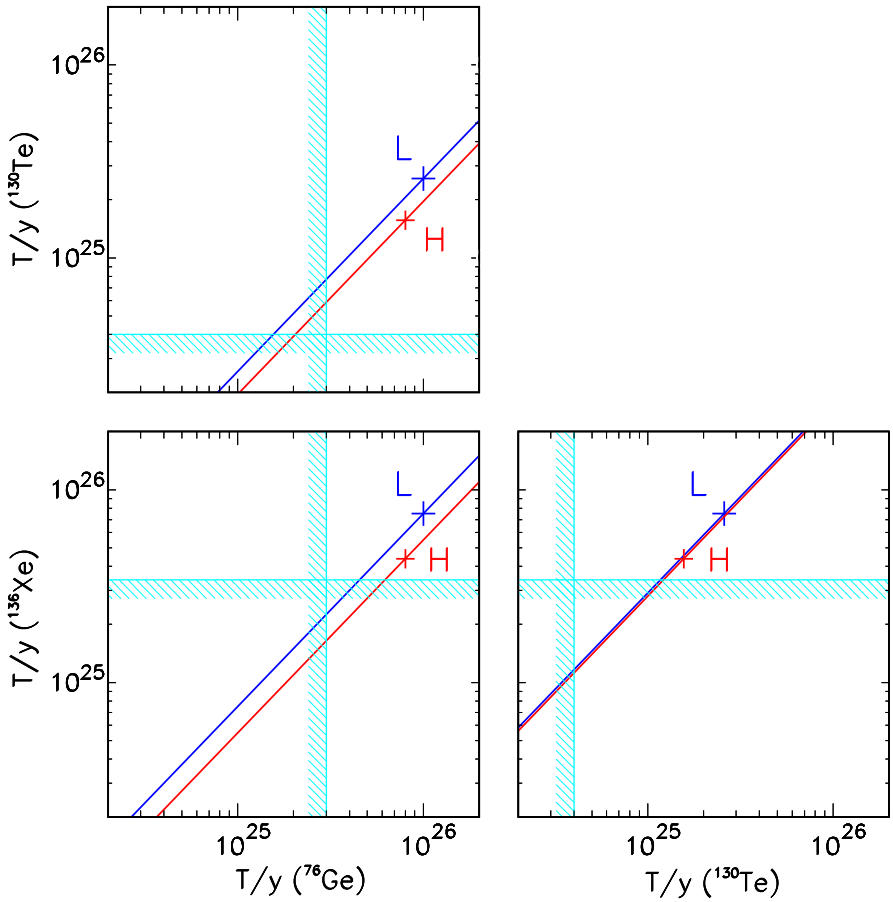

FIG. 3 (color online). Correlation plot of expected half-lives in different pairs of nuclei (slanted lines) together with residual theoretical errors (crosses) for the L and H decay mechanisms (blue and red lines, respectively). Also shown are the current experimental limits, as reported in Table I. See the text for details.

indistinguishability of the L and H mechanisms, which is especially evident in the rightmost panel, where the half-life expectations for the L and H cases are almost coincident. In the other two panels on the left, the L and H lines are visually separated, but they can overlap within error bars. As far as the separation between the slanted lines in Fig. 3 remains smaller than or comparable to the theoretical error bars, future experimental data on the half-lives (no matter how accurate) will not be able to tell the L from the H mechanism. In the following section, we shall quantify the two kinds of degeneracies by performing an analysis of prospective data.

IV. STATISTICAL ANALYSIS OF PROSPECTIVE $0\nu\beta\beta$ DATA

There are good prospects to improve the current limits (Table I) on the $0\nu\beta\beta$ half-life in the candidate nuclei (^{76}Ge, ^{130}Te, ^{136}Xe). In particular, in the next decade, upgrades of the current experiments or new planned projects should be able to explore an additional order of magnitude in T_i [2–5] and hopefully find evidence for the decay. Below, we shall optimistically assume that a $0\nu\beta\beta$ decay signal is found in each of the three nuclei.

A. Reference scenario

We assume that the measured ^{76}Ge half-life takes a reference value of 10^{26} y. The half-lives for ^{130}Te and ^{136}Xe in the L and H mechanisms are then obtained via Eq. (19). We also assume that each T_i is measured within $\pm 20\%$ at 1σ, corresponding to ± 0.08 accuracy on τ_i. Our prospective data sets are thus given by the following central values and errors ($\bar{\tau}_i^j \pm s_i^j$) for the L and H cases, respectively:

$$\text{data set}(L) \Leftrightarrow \begin{cases} \bar{\tau}_1^L \pm s_1^L = 26.000 \pm 0.080, \\ \bar{\tau}_2^L \pm s_2^L = 25.412 \pm 0.080, \\ \bar{\tau}_3^L \pm s_3^L = 25.875 \pm 0.080, \end{cases} \tag{20}$$

$$\text{data set}(H) \Leftrightarrow \begin{cases} \bar{\tau}_1^H \pm s_1^H = 26.000 \pm 0.080, \\ \bar{\tau}_2^H \pm s_2^H = 25.292 \pm 0.080, \\ \bar{\tau}_3^H \pm s_3^H = 25.739 \pm 0.080. \end{cases} \tag{21}$$

Figure 4 shows the above data sets (black dots with crossed error bars) overlaid on the same theoretical predictions (colored slanted lines with errors) for the L and H cases as in Fig. 3. We discuss below the implications of these data on the degeneracy issues, by means of a statistical analysis.

B. Degeneracy between LNV parameter and QRPA uncertainties for fixed $0\nu\beta\beta$ decay mechanism

Let us assume one of the two Majorana neutrino exchange mechanisms (either L or H) as the "true" one for the $0\nu\beta\beta$ decay in the three nuclei. Given the previous QRPA calculations, the prospective data sets, and their associated uncertainties, we aim at determining the associated LNV parameter (either μ^L or μ^H) and its errors.

To this purpose, we consider the following χ^2 function in terms of the "rescaled" parameter $\bar{\mu}^j$ in Eq. (18),

$$\chi^2(\bar{\mu}^j) = \sum_{i=1}^{3} \frac{(\tau_i - \bar{\tau}_i^j)^2}{(s_i^j)^2 + (2\sigma^j)^2} = \sum_{i=1}^{3} \frac{(\gamma_i - 2\bar{\eta}_i^j - 2\bar{\mu}^j - \bar{\tau}_i)^2}{(s_i^j)^2 + (2\sigma^j)^2}. \quad (22)$$

Minimization of χ^2 provides the central value $\bar{\mu}_c^j$ (at $\chi^2 = 0$, by construction) and its error δ^j (at $\Delta\chi^2 = 1$). We get

$$\bar{\mu}_c^j \pm \delta^j = \begin{cases} -0.772 \pm 0.029(L), \\ -2.572 \pm 0.027(H). \end{cases} \quad (23)$$

The LNV parameter μ^j is then obtained from Eq. (18) as

$$\mu^j = \bar{\mu}_c^j - \alpha^j(g_A - 1) - s\beta^j \pm \delta^j. \quad (24)$$

The above expression for μ^j provides a useful breakdown of its uncertainties: from left to right, the terms following the central value $\bar{\mu}_c^j$ represent, respectively, the systematic error due to g_A variations from the unit value, the systematic bias due to the choice of the nucleon-nucleon potential (CD-Bonn vs Argonne), and the residual error from theory and data uncertainties.

Figure 5 represents the results of the above statistical analysis, in terms of the LNV parameters $m_{\beta\beta}$ and $M_{\beta\beta}$ associated to the L and H mechanisms, as defined in Eqs. (6) and (7), respectively. The LNV parameters are shown (in logarithmic scale) as a function of g_A, whose variation in the representative range $g_A \in [0.8, 1.27]$

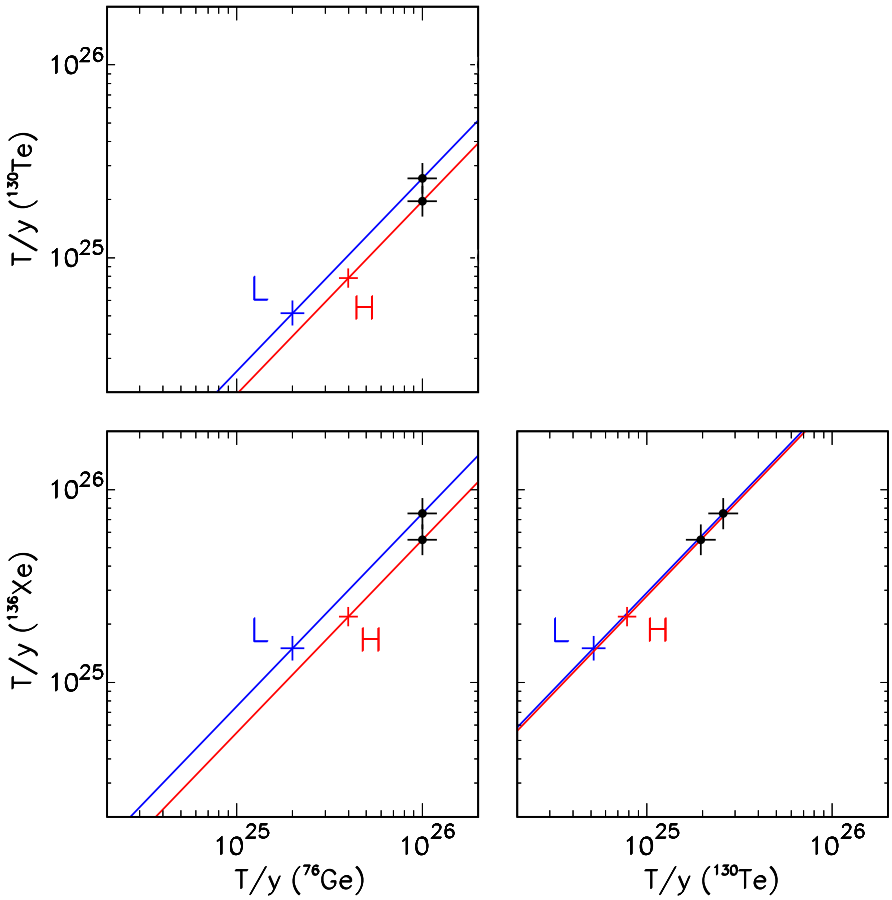

FIG. 4 (color online). As in Fig. 3, but with lower limits replaced by prospective determinations of the half-lives (black dots and crosses). See the text for details.

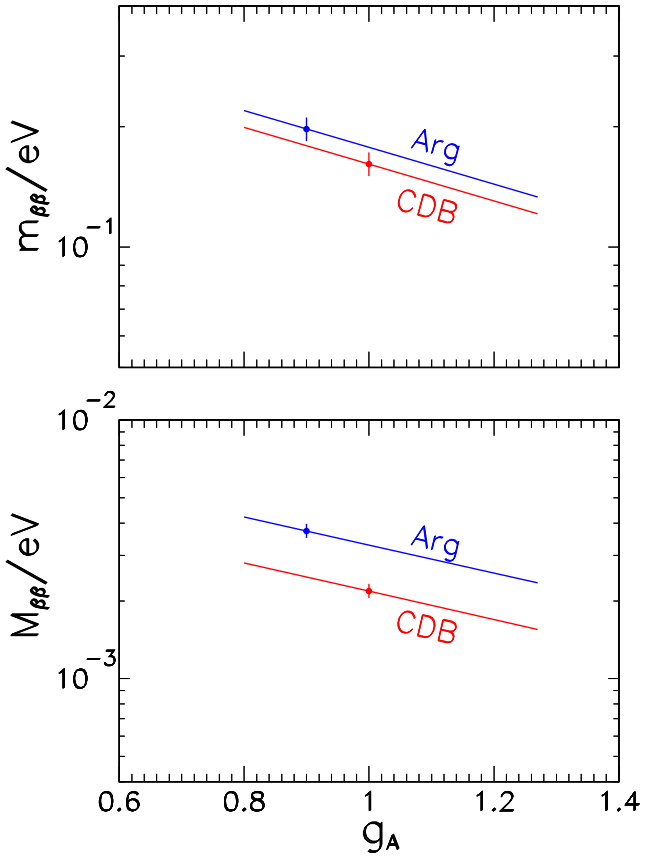

FIG. 5 (color online). Upper panel: Light (L) Majorana neutrino exchange mechanism. The LNV parameters $m_{\beta\beta}$ (in eV), as derived from a fit to the prospective data in Eq. (20), is shown as a function of g_A (in the range $g_A \in [0.8, 1.27]$). The two curves refer to the CD-Bonn and Argonne choices for the nucleon-nucleon potential. The error bars attached to each line mark the size of the residual theoretical and experimental uncertainties from the fit. Lower panel: as above, but for heavy (H) Majorana neutrino exchange with LNV parameter $M_{\beta\beta}$, from a fit to the prospective data in Eq. (21).

induces the main source of uncertainty: the higher g_A, the smaller $m_{\beta\beta}$ or $M_{\beta\beta}$. In decreasing order of relevance, the second source of uncertainty is represented by the nucleon-nucleon potential, whose twofold option (CD-Bonn vs Argonne) splits the LNV parameter estimates into two curves. Finally, the third and smallest source of uncertainties is induced by δ^j [see Eq. (24)] and is shown as a representative error bar, on top of each curve. The total uncertainty affecting each LNV parameter is given by the "envelope" of all these errors which, for $g_A \in [0.80, 1.27]$, amounts to a factor of $\sim$2 for $m_{\beta\beta}$, and to a factor of $\sim$3 for $M_{\beta\beta}$ (from minimum to maximum, in both cases).

Overall uncertainties of a factor $\sim$2 in the reconstructed value of $m_{\beta\beta}$ are definitely large, but not as dramatic as those of $O(10)$ discussed in [30,35]. This feature of the QRPA approach may thus be of interest for relatively robust estimates of the experimental sensitivity to $m_{\beta\beta}$. We stress that, as mentioned in Sec. III B, in the QRPA the effective dependence of the NME on the g_A parameter ($M_i^j \sim g_A$) is milder than in other frameworks (where $M_i^j \sim g_A^2$), as a result of the stabilizing role of the "$2\nu\beta\beta$ calibration" of the g_{pp} parameter.

In any case, limiting the g_A range in Fig. 5, by means of dedicated theoretical and experimental studies, will be a major step towards the reduction of the reconstructed LNV parameter uncertainties. One should also refine the understanding of the nucleon-nucleon potential, so as to bring the two splitted curves in Fig. 5 closer to each other. Such a long-term nuclear modeling program, although rather challenging, is warranted by the fundamental importance of the worldwide $0\nu\beta\beta$ decay search program.

C. Degeneracy between light and heavy neutrino exchange mechanisms for $0\nu\beta\beta$ decay

As already mentioned, the ensembles of expected half-lives for the L and H mechanisms (slanted lines in Fig. 3) are very close to each other, as compared to current theoretical uncertainties and prospective experimental errors (see Fig. 4). This fact suggests that the two mechanisms are largely degenerate; i.e., they cannot be distinguished by data from the three candidate nuclei considered herein. One can quantify the degree of degeneracy as follows: the prospective data for one mechanism (say, L) are fitted with the predictions of the other mechanism (say, H), and vice versa. The value of $\chi^2_{\rm min}$ quantifies then the "degree of misfit": the lower is $\chi^2_{\rm min}$, the more difficult is to distinguish the L and H mechanisms. By using a χ^2 approach as in Eq. (22), we find that, as expected, the misfit is not statistically significant: $\chi^2_{\rm min} \simeq 1.1$ in both cases. Therefore, the two mechanisms are phenomenologically indistinguishable at the level of $(\chi^2_{\rm min})^{1/2} \sim 1\sigma$.

It should be noted that this small 1σ difference between the L and H scenarios is generated solely by the smallest sources of uncertainties (the data errors s_i^j and the residual theoretical errors σ^j), while it does not depend on the value of g_A or on the choice of the nucleon-nucleon potential (which can be absorbed by variations of the unknown LNV parameter λ_j in the fit). Improving the latter two sources of uncertainties, despite being crucial to assess λ_j, would not help to lift the L-H mechanism degeneracy. Breaking the degeneracy would require the challenging reduction of the nonparametric component of the theoretical error σ^j (which is at the level of $10^{\sigma_j} \simeq 5\%$–7% in our approach) and of the prospective experimental errors s_j^i (which we have assumed to be at the $\simeq$20% level in this work).

It is not obvious how the above stringent requirements can be achieved, even in the far future. In any case, we remind the reader that such conclusions refer to the specific decay mechanisms, candidate nuclei, and QRPA nuclear model considered in this work and might, thus, be altered in

a wider context. In general, favorable cases for the discrimination of any two decay mechanisms in a pair of candidate nuclei can be diagnosed, via correlation plots analogous to our Figs. 1 and 3, by the emergence of a significant "transverse" separation of the slanted error bands (see also [20,23]).

V. SUMMARY

We have studied in detail a phenomenological scenario involving three candidate nuclei for $0\nu\beta\beta$ decay (^{76}Ge, ^{130}Te, ^{136}Xe), two representative particle physics mechanisms (light and heavy Majorana neutrino exchange, with LNV parameters $m_{\beta\beta}$ e $M_{\beta\beta}$), and a large set of nuclear matrix elements, computed within the quasiparticle random phase approximation. We have found that the main theoretical uncertainties, induced by the effective axial coupling g_A and with the nucleon-nucleon potential, can be parametrized in terms of rescaling factors for the nuclear matrix elements, up to small residuals. Within the QRPA, the effective rescaling induced by g_A variations is found to be almost linear, rather than quadratic in g_A as naively expected. Despite this favorable feature, we find that, in each mechanism, the relevant lepton number violation parameter is largely degenerate with the rescaling factors; in particular, for $g_A \in [0.8, 1.27]$ the total $m_{\beta\beta}$ ($M_{\beta\beta}$) uncertainty in numerical experiments amounts to a factor of about two (three). Moreover, the light and heavy neutrino exchange mechanisms turn out to be largely indistinguishable from a phenomenological viewpoint. The stringent conditions needed to lift the degeneracies between particle and nuclear physics aspects of $0\nu\beta\beta$ decay have been briefly discussed. Progress may be envisaged, on the one hand, by studying further decay mechanisms and candidate nuclei and, on the other hand, by understanding the various theoretical uncertainties associated to the QRPA and other nuclear models, and especially the effective functional dependence of the matrix elements on g_A.

ACKNOWLEDGMENTS

The work of E. L. is supported by the Italian Istituto Nazionale di Fisica Nucleare (INFN) and Ministero dell'Istruzione, dell'Università e della Ricerca (MIUR) through the "Astroparticle Physics" research projects. The work of and A. M. R. is supported by MIUR. F. Š. acknowledges support by the VEGA Grant Agency of the Slovak Republic under Contract No. N. 1/0876/12.

[1] K. A. Olive *et al.* (Particle Data Group), Review of particle physics, Chin. Phys. C **38**, 090001 (2014), and see therein the review "Neutrinoless double-β decay," by P. Vogel and A. Piepke.
[2] S. R. Elliott, Recent progress in double beta decay, Mod. Phys. Lett. A **27**, 1230009 (2012).
[3] B. Schwingenheuer, Status and prospects of searches for neutrinoless double beta decay, Ann. Phys. (Berlin) **525**, 269 (2013).
[4] O. Cremonesi and M. Pavan, Challenges in double beta decay, Adv. High Energy Phys. **2014**, 951432 (2014).
[5] J. J. Gómez-Cadenas and J. Martín-Albo, Phenomenology of neutrinoless double beta decay, arXiv:1502.00581.
[6] S. T. Petcov, The nature of massive neutrinos, Adv. High Energy Phys. **2013**, 852987 (2013).
[7] W. Rodejohann, Neutrino-less double beta decay and particle physics, Int. J. Mod. Phys. E **20**, 1833 (2011).
[8] J. D. Vergados, H. Ejiri, and F. Simkovic, Theory of neutrinoless double beta decay, Rep. Prog. Phys. **75**, 106301 (2012).
[9] F. F. Deppisch, M. Hirsch, and H. Päs, Neutrinoless double beta decay and physics beyond the standard model, J. Phys. G **39**, 124007 (2012).
[10] S. M. Bilenky and C. Giunti, Neutrinoless double-beta decay: A probe of physics beyond the standard model, Int. J. Mod. Phys. A **30**, 1530001 (2015).
[11] F. Deppisch and H. Pas, Pinning Down The Mechanism of Neutrinoless Double Beta Decay with Measurements in Different Nuclei, Phys. Rev. Lett. **98**, 232501 (2007).
[12] V. M. Gehman and S. R. Elliott, Multiple-isotope comparison for determining $0\nu\beta\beta$ mechanisms, J. Phys. G **34**, 667 (2007); **35**, 029701(E) (2008).
[13] G. L. Fogli, E. Lisi, and A. M. Rotunno, Probing particle and nuclear physics models of neutrinoless double beta decay with different nuclei, Phys. Rev. D **80**, 015024 (2009).
[14] F. Simkovic, J. Vergados, and A. Faessler, Few active mechanisms of the neutrinoless double beta-decay and effective mass of Majorana neutrinos, Phys. Rev. D **82**, 113015 (2010).
[15] A. Faessler, A. Meroni, S. T. Petcov, F. Simkovic, and J. Vergados, Uncovering multiple CP-nonconserving mechanisms of $\beta\beta$-decay, Phys. Rev. D **83**, 113003 (2011).
[16] A. Ali, A. V. Borisov, and D. V. Zhuridov, Neutrinoless double beta decay: Searching for new physics with comparison of different nuclei, in *Proceedings of the 14th Lomonosov Conference on Elementary Particle Physics, Moscow, Russia, 2009*, edited by A. I. Studenikin (World Scientific, Singapore, 2011), p. 168.
[17] A. Faessler, G. L. Fogli, E. Lisi, V. Rodin, A. M. Rotunno, and F. Simkovic, QRPA uncertainties and their correlations in the analysis of $0\nu\beta\beta$ decay, Phys. Rev. D **79**, 053001 (2009).

[18] A. Faessler, G. L. Fogli, E. Lisi, V. Rodin, A. M. Rotunno, and F. Simkovic, Addendum to: Quasiparticle random phase approximation uncertainties and their correlations in the analysis of $0\nu\beta\beta$ decay, Phys. Rev. D **87**, 053002 (2013).
[19] J. Engel, Uncertainties in nuclear matrix elements for neutrinoless double-beta decay, J. Phys. G **42**, 034017 (2015).
[20] A. Faessler, G. L. Fogli, E. Lisi, A. M. Rotunno, and F. Simkovic, Multi-isotope degeneracy of neutrinoless double beta decay mechanisms in the quasi-particle random phase approximation, Phys. Rev. D **83**, 113015 (2011).
[21] M. Mitra, G. Senjanovic, and F. Vissani, Neutrinoless double beta decay and heavy sterile neutrinos, Nucl. Phys. **B856**, 26 (2012).
[22] M. Horoi, Shell model analysis of competing contributions to the double-β decay of ^{48}Ca, Phys. Rev. C **87**, 014320 (2013).
[23] A. Meroni, S. T. Petcov, and F. Simkovic, Multiple CP non-conserving mechanisms of $\beta\beta$-decay and nuclei with largely different nuclear matrix elements, J. High Energy Phys. 02 (2013) 025.
[24] S. Pascoli, M. Mitra, and S. Wong, Effect of cancellation in neutrinoless double beta decay, Phys. Rev. D **90**, 093005 (2014).
[25] P. S. Bhupal Dev, S. Goswami, M. Mitra, and W. Rodejohann, Constraining neutrino mass from neutrinoless double beta decay, Phys. Rev. D **88**, 091301 (2013).
[26] F. Osterfeld, Nuclear spin and isospin excitations, Rev. Mod. Phys. **64**, 491 (1992).
[27] P. Vogel, Nuclear structure and double beta decay, J. Phys. G **39**, 124002 (2012).
[28] A. Faessler, G. L. Fogli, E. Lisi, V. Rodin, A. M. Rotunno, and F. Simkovic, Overconstrained estimates of neutrinoless double beta decay within the QRPA, J. Phys. G **35**, 075104 (2008).
[29] J. Suhonen and O. Civitarese, Probing the quenching of g_A by single and double beta decays, Phys. Lett. B **725**, 153 (2013).
[30] J. Barea, J. Kotila, and F. Iachello, Nuclear matrix elements for double-β decay, Phys. Rev. C **87**, 014315 (2013).
[31] N. Yoshida and F. Iachello, Two neutrino double-β decay in the interacting boson-fermion model, Prog. Theor. Exp. Phys. **2013**, 043D01 (2013).
[32] J. Barea, J. Kotila, and F. Iachello, $0\nu\beta\beta$ and $2\nu\beta\beta$ nuclear matrix elements in the interacting boson model with isospin restoration, Phys. Rev. C **91**, 034304 (2015).
[33] J. Menendez, D. Gazit, and A. Schwenk, Chiral Two-Body Currents in Nuclei: Gamow-Teller Transitions and Neutrinoless Double-Beta Decay, Phys. Rev. Lett. **107**, 062501 (2011).
[34] R. G. H. Robertson, Empirical survey of neutrinoless double beta decay matrix elements, Mod. Phys. Lett. A **28**, 1350021 (2013).
[35] S. Dell'Oro, S. Marcocci, and F. Vissani, New expectations and uncertainties on neutrinoless double beta decay, Phys. Rev. D **90**, 033005 (2014).
[36] F. Vissani, La Thuile 2014: Theoretical premises to neutrino round table, Nuovo Cimento C **037**, 66 (2014).
[37] V. A. Rodin, A. Faessler, F. Simkovic, and P. Vogel, Assessment of uncertainties in QRPA $0\nu\beta\beta$-decay nuclear matrix elements, Nucl. Phys. **A766**, 107 (2006); **793**, 213(E) (2007).
[38] F. Simkovic, R. Hodak, A. Faessler, and P. Vogel, Relation between the $0\nu\beta\beta$ and $2\nu\beta\beta$ nuclear matrix elements revisited, Phys. Rev. C **83**, 015502 (2011).
[39] J. Engel, F. Simkovic, and P. Vogel, Chiral two-body currents and neutrinoless double-beta decay in the QRPA, Phys. Rev. C **89**, 064308 (2014).
[40] A. Halprin, S. T. Petcov, and S. P. Rosen, Effects of light and heavy majorana neutrinos in neutrinoless double beta decay, Phys. Lett. **125B**, 335 (1983).
[41] F. Simkovic, G. Pantis, J. D. Vergados, and A. Faessler, Additional nucleon current contributions to neutrinoless double beta decay, Phys. Rev. C **60**, 055502 (1999).
[42] A. Faessler, M. Gonzalez, S. Kovalenko, and F. Simkovic, Arbitrary mass Majorana neutrinos in neutrinoless double beta decay, Phys. Rev. D **90**, 096010 (2014).
[43] J. Kotila and F. Iachello, Phase space factors for double-β decay, Phys. Rev. C **85**, 034316 (2012).
[44] M. Agostini *et al.* (GERDA Collaboration), Results on Neutrinoless Double-β Decay of ^{76}Ge from Phase I of the GERDA Experiment, Phys. Rev. Lett. **111**, 122503 (2013).
[45] C. E. Aalseth *et al.* (IGEX Collaboration), The IGEX ^{76}Ge neutrinoless double beta decay experiment: Prospects for next generation experiments, Phys. Rev. D **65**, 092007 (2002).
[46] H. V. Klapdor-Kleingrothaus, A. Dietz, L. Baudis, G. Heusser, I. V. Krivosheina, S. Kolb, B. Majorovits, H. Päs *et al.*, Latest results from the Heidelberg-Moscow double beta decay experiment, Eur. Phys. J. A **12**, 147 (2001).
[47] K. Alfonso *et al.* (CUORE Collaboration), Search for Neutrinoless Double-Beta Decay of ^{130}Te with CUORE-0, Phys. Rev. Lett. **115**, 102502 (2015).
[48] E. Andreotti, C. Arnaboldi, F. T. Avignone, M. Balata, I. Bandac, M. Barucci, J. W. Beeman, F. Bellini *et al.*, ^{130}Te neutrinoless double-beta decay with CUORICINO, Astropart. Phys. **34**, 822 (2011).
[49] A. Gando *et al.* (KamLAND-Zen Collaboration), Limit on Neutrinoless $\beta\beta$ Decay of ^{136}Xe from the First Phase of KamLAND-Zen and Comparison with the Positive Claim in ^{76}Ge, Phys. Rev. Lett. **110**, 062502 (2013).
[50] M. Auger *et al.* (EXO Collaboration), Search for Neutrinoless Double-Beta Decay in ^{136}Xe with EXO-200, Phys. Rev. Lett. **109**, 032505 (2012).
[51] F. Simkovic, A. Faessler, V. Rodin, P. Vogel, and J. Engel, Anatomy of nuclear matrix elements for neutrinoless double-beta decay, Phys. Rev. C **77**, 045503 (2008).
[52] F. Simkovic, A. Faessler, H. Muther, V. Rodin, and M. Stauf, The $0\nu\beta\beta$-decay nuclear matrix elements with self-consistent short-range correlations, Phys. Rev. C **79**, 055501 (2009).
[53] F. Simkovic, V. Rodin, A. Faessler, and P. Vogel, $0\nu\beta\beta$ and $2\nu\beta\beta$ nuclear matrix elements, quasiparticle random-phase approximation, and isospin symmetry restoration, Phys. Rev. C **87**, 045501 (2013).
[54] S. J. Freeman and J. P. Schiffer, Constraining the $0\nu2\beta$ matrix elements by nuclear structure observables, J. Phys. G **39**, 124004 (2012).